

Pressure-induced electronic and structural phase transitions in solid hydrogen

B. I. Min and H. J. F. Jansen*

Department of Physics and Astronomy, Northwestern University, Evanston, Illinois 60201

A. J. Freeman

*Department of Physics and Astronomy, Northwestern University, Evanston, Illinois 60201
and Center for Materials Science, Los Alamos National Laboratory, Los Alamos, New Mexico 87545*

(Received 2 December 1985)

Possible induced electronic and structural phase transitions in solid hydrogen are studied using a unified theoretical approach—the local-density total-energy full-potential linearized-augmented-plane-wave method—which has the precision to treat the highly anisotropic Pa_3 molecular phase on the same footing as the monatomic close-packed phases. The pressure-induced metallization by band overlap and bond length relaxation within the Pa_3 structure of molecular solid hydrogen is described and discussed; the calculations predict an insulator-to-metal phase transition at 1.7 ± 0.2 Mbar. At a much higher pressure of 4 ± 1 Mbar, a structural phase transition takes place to a monatomic metallic hcp phase with a high superconducting transition temperature.

I. INTRODUCTION

The possibility of a metal-insulator phase transition in solid hydrogen at high pressure has been the focus of considerable research ever since Wigner and Huntington¹ proposed that a structural transition from a diatomic molecular phase (which is the stable phase at normal conditions) to a monatomic metallic phase might occur. Obviously, in order to obtain reliable information about the existence of this transition, a careful study of the thermodynamics of both phases should be performed. Only then will it be possible to predict the structural transition pressure and the corresponding equation of state. The accuracy of most previous theoretical investigations of the electronic structure, however, was limited because different approximations had to be invoked for the diatomic and monatomic phases, because of the large difference in crystal structure of molecular and atomic hydrogen. In this paper we report the results of our unified approach for both crystal structures and a precise comparison establishes the existence of the structural phase transition.

Diatomic molecular solid hydrogen has a number of features which are different from those of other molecular solids. Most importantly, the rotational motion of the isolated molecules is not suppressed even in the solid because of the small moment of inertia. Because of this rotational degree of freedom, molecular hydrogen appears in two different modifications, parahydrogen and orthohydrogen, which have even ($J=0$) and odd ($J=1$) rotational quantum numbers, respectively. The stable ground state is para-H, but the energy difference from ortho-H is only 170.5 K (~ 1.1 mRy or 15 meV). At low temperatures, ortho-H shows an order-disorder phase transition in which the long axis of the molecules align along specific crystalline directions. Much work was devoted to this orientational ordering in the past decade² in an attempt to understand the phase transition and ground-state structure. It is generally accepted that the ordered ground state of ortho-H has a Pa_3 space-group structure with four molecules per unit cell (see Fig. 1). The molecular

centers are located on the sites of an fcc lattice and the molecular axes are oriented along specific body diagonals. This configuration has the lowest energy for a three-dimensional arrangement of $J=1$ molecules interacting through electric quadrupole-quadrupole (EQQ) interactions. Parahydrogen, which has a spherically symmetric distribution of molecular axes, is also expected to have an orientationally ordered phase at high pressure due to the increased effect of anisotropic molecular interactions. We

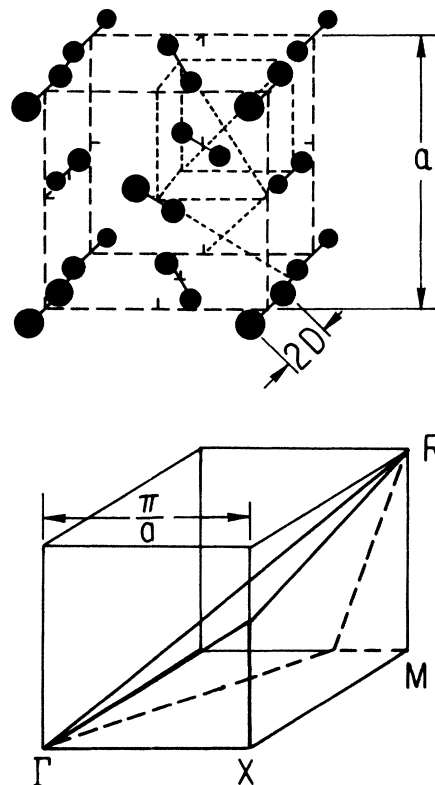


FIG. 1. Pa_3 structure and its $\frac{1}{24}$ irreducible Brillouin zone of molecular solid hydrogen. a is the lattice constant and $2D$ is the molecular bond length.

therefore assume the structure of static diatomic molecular hydrogen to be Pa_3 .

Our theoretical approach to investigate the structural transition is to calculate the total energy of both phases using a very precise local-density band-structure method. The structure of Pa_3 molecular hydrogen is very anisotropic in contrast to the case of monatomic metallic hydrogen. For a precise description of the charge density in this open, anisotropic structure, a full-potential band-structure method (in which no shape approximations to either the density or the potential are made) is essential. We performed total-energy calculations for both diatomic and monatomic solid hydrogen using our full-potential linearized-augmented-plane-wave (FLAPW) band-structure method³ within the local density approximation (LDA). Since in the FLAPW method the large anisotropic molecular interactions of molecular hydrogen can be treated precisely, a direct and consistent comparison of the total energies of both phases is possible. Combining the results for monatomic metallic hydrogen, which were reported in a previous paper,⁴ and the results for the electronic structure and total energy of diatomic molecular hydrogen (as studied in this paper), we arrive at a consistent description of the structural and corresponding metal-insulator phase transitions between the two phases. We also investigate the pressure-induced metallization by band overlap and bond relaxation within the Pa_3 structure of molecular solid hydrogen. A similar transition is observed⁵ in the comparable molecular solid I_2 . It should be kept in mind that our band structure and total energy calculations are done at $T=0$. Thus we investigate, in this paper, the Gibb's free energy without the inclusion of the entropy contribution; this latter can, in principle, be included later on for the complete description of phase transition.

The methods we have used are briefly presented in Sec. II, and the results of our band structure and total energy calculations for molecular solid hydrogen are given in Sec. III. Structural transitions are discussed in Sec. IV and, finally, we give a discussion and summary in Sec. V. Numerical details are found in the Appendix.

II. METHOD

For the band-structure calculations of molecular solid hydrogen, we use the self-consistent FLAPW method³ in which one makes no shape approximations to the potential or the charge density. For convenience, the unit cell is divided into two distinct regions of space in a standard way by surrounding the atomic nuclei with so-called muffin-tin spheres. The potential (and charge density) in the two regions is expanded in spherical harmonics and plane waves, respectively:

$$\begin{aligned} V(\mathbf{r}) &= \sum_{l,m} V_{lm}(r) Y_{lm}(\hat{\mathbf{r}}) \quad (\text{inside spheres}) \\ &= \sum_{\mathbf{G}} V(\mathbf{G}) \exp(i\mathbf{G}\cdot\mathbf{r}) \quad (\text{interstitial}). \end{aligned} \quad (1)$$

The introduction of muffin-tin spheres is a purely numerical construction which facilitates the calculation because it allows the potential (and charge density) to be represent-

ed by two rapidly converging series. If we consider only the first terms in each series, we recover the muffin-tin approximation. This approximation is reasonable for close-packed metals, but it breaks down severely in materials with an open structure like solid molecular hydrogen.

In solving the effective one-electron Kohn-Sham equations,⁶ we use the local density approximation for the exchange and correlation potential as given by Hedin and Lundqvist.⁷ The total energy per unit cell is given by⁸

$$\begin{aligned} E &= \sum \epsilon_i - \frac{1}{2} \int_{\Omega} n(r) V_C(r) d^3r \\ &\quad - \int_{\Omega} n(r) [V_{xc}(r) - \epsilon_{xc}(r)] d^3r - \frac{1}{2} \sum_{\nu} Z_{\nu} V_M(r_{\nu}), \end{aligned} \quad (2)$$

where Z_{ν} , ϵ_i , and $n(r)$ are the nuclear charge, eigenvalues, and charge density. $V_C(r)$, $V_{xc}(r)$, and $V_M(r)$ denote the Coulomb, exchange-correlation, and Madelung potentials and ϵ_{xc} is the exchange correlation energy.

It needs to be re-emphasized that because all contributions to the potential and charge density are completely taken into account in this full-potential approach, it is possible to treat the highly anisotropic nature of the interactions in solid molecular hydrogen with the same level of precision as was done for the metallic interactions in monatomic hydrogen. Since the FLAPW method does not contain uncontrolled numerical parameters,³ it allows one to obtain well converged results using analytical convergence rules (see Appendix). As a result, the only approximation influencing our final results is connected to the use of the LDA itself.

III. BAND STRUCTURE AND TOTAL ENERGY

We have performed self-consistent band-structure calculations on solid molecular hydrogen in the Pa_3 space-group structure. The basic Bravais lattice of this structure is simple cubic with four molecules per unit cell. The periodic potential and charge density were expanded with up to 6043 plane waves in the interstitial region and with l up to 4 (which includes 9 Kubic harmonics) inside the spheres. The Bloch eigenfunctions were expanded with up to 751 LAPW basis functions. In the self-consistent iterations, energy eigenvalues were calculated for 80 k points in the $(\frac{1}{24})$ th irreducible Brillouin zone (see Fig. 1).

Next we consider the total energy for the case where we keep the interproton length $2D$ fixed at the free molecule's bond length. It is this very small bond length that determines the maximum size of the muffin-tin radius. When it is small compared with the intermolecular distance (i.e., when D/a small, with a the lattice constant), the computational problem becomes numerically exceedingly difficult. This results in a lower precision of the total energy in the low-density region. In this case, where we have a large lattice constant, we need many plane waves to describe properly the charge density and potential in the large interstitial region. For example, we should use 5800 LAPW basis functions at $r_s = 3.1$ in order to get the same level of precision as in the case of $r_s = 1.0$, which is clearly impossible. (Here r_s is the Wigner-Seitz radius in a.u.,

characterizing the density as defined by $4\pi r_s^3/3=1/n$, where n is the electron number density). On the other hand, the dependence of the total energy on the number of k points is minimal in this low-density region, where the material is an insulator. The situation is reversed in the high-density metallic region, where a very large number of k points is required.⁴ This makes the application of the FLAPW method to solid molecular hydrogen more difficult compared to the other molecular solids which have larger values of D/a . Detailed convergence tests are presented in the Appendix. As a result of this problem, the numerical errors in the total energy in the low-density insulating region are rather large compared with those in the high-density metallic region. For example, while ΔE is about 20 mRy at $r_s=3.1$ a.u., the numerical errors in the total energy in the high-density metallic region, in which the structural transition occurs, are less than 1 mRy, which is sufficient for our needs.

Figure 2 shows the band structure of molecular solid hydrogen at the experimental lattice constant, $r_s=3.1$ a.u. The overall shape of the band structure is similar to that of Friedli and Ashcroft.⁹ The energy gap between the valence and conduction bands, 9.3 ± 0.3 eV, is close to that of Friedli and Ashcroft (9.2 eV) but is much smaller than the experimental value or that of a Hartree-Fock calculation.¹⁰ The absorption spectrum¹¹ of solid H_2 exhibits two broad structures at about 12.5 and 17 eV; the first peak has been interpreted as an exciton transition and the latter as an interband transition. This discrepancy is expected since the LDA usually underestimates the value of the energy gap.

The band structure at a much smaller lattice constant ($r_s=1.5$), cf. Fig. 3, shows the mechanism for metallization by band overlap under pressure within the Pa_3 structure. With decreasing lattice constant, the indirect energy gap between the eigenvalues at R and X becomes smaller and smaller until finally a band overlap occurs. Figure 4 provides the size of the energy gap as a function of r_s . Band overlap sets in at $r_s=1.44$ a.u. corresponding to a pressure of about 1.7 Mbar. This metallization mechanism is similar to that in I_2 , in which an insulator-metal

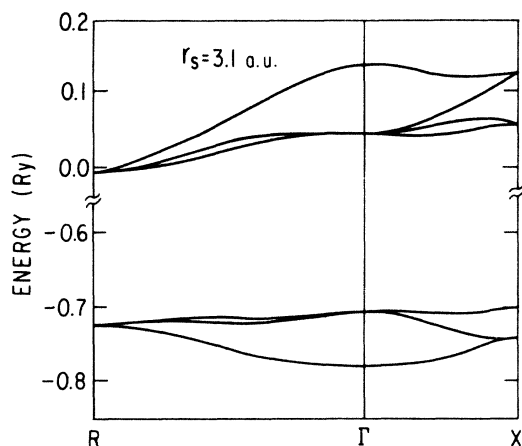


FIG. 2. Band structure of Pa_3 molecular solid hydrogen at $r_s=3.1$ a.u.

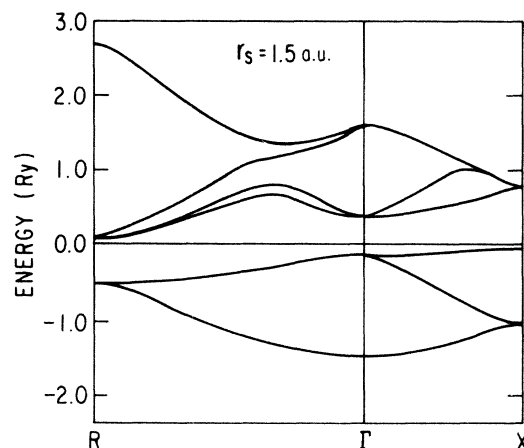


FIG. 3. Band structure of Pa_3 molecular solid hydrogen at $r_s=1.5$ a.u.

transition also occurs without structural change.⁵

The results of our total energy calculations as a function of r_s are given in Fig. 5. The minimum in the total energy curve is located at $r_s=2.5(\pm 0.1)$ a.u.; the error given is rather large due to the large numerical error in the low-density region. Our value is larger than that of Chakravarty *et al.*¹² ($r_s=2.1$ a.u.), but it is still much smaller than the experimental value ($r_s=3.1$ a.u.). This large discrepancy finds its origin in the assumption of a static crystal structure. We have calculated the band structure of Pa_3 molecular hydrogen with orientationally ordered molecular axes, whereas the real structure is solid para- H_2 with almost freely rotating molecules. Because of these rotations, ground-state solid parahydrogen at normal pressure behaves like solid helium with isotropic in-

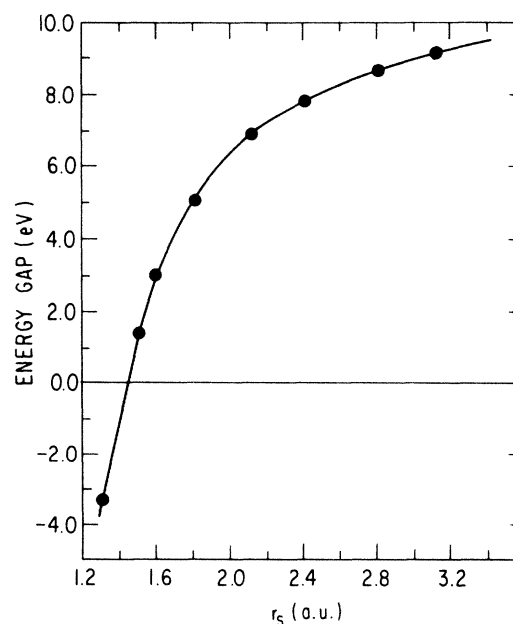


FIG. 4. Band gap of Pa_3 molecular solid hydrogen (energy difference between eigenvalues at R and X) as a function of r_s .

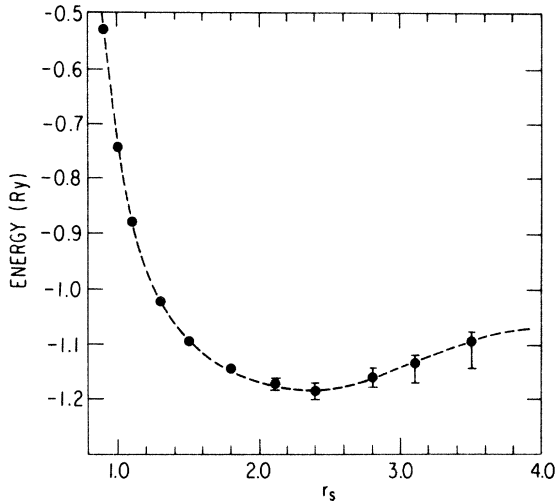


FIG. 5. Total energy of Pa_3 molecular solid hydrogen per proton as a function of r_s .

interactions between the rotating molecules.² We can simulate this isotropic intermolecular interaction by retaining only the spherical term¹³ in the multipole expansion of the potential. In this way, we obtain the equilibrium density $r_s = 3.15$ a.u., which is close to the experimental value. The total energy (-1.047 Ry), however, is rather high in this case, since the anisotropic interactions are not considered. This result indicates that the molecular axes of solid para-H at normal pressure do not order and hence that a direct comparison of our calculated quantities with experiment at low pressures is not possible. In the following sections we focus on the high-pressure region where even para-H orders orientationally and where the rotational degrees of freedom do not play a significant role.

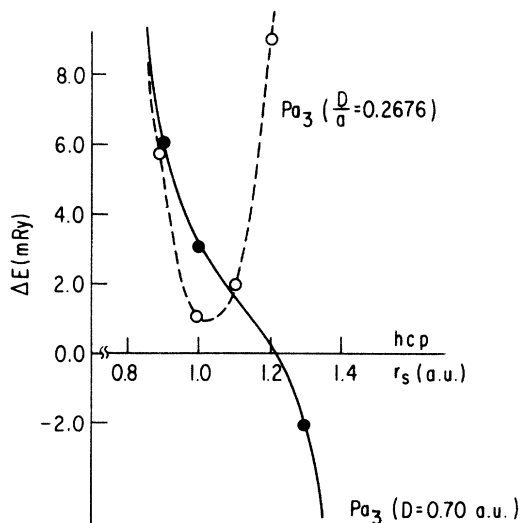


FIG. 6. Total energy of diatomic hydrogen relative to hcp monatomic hydrogen. The solid line corresponds to the energy with fixed bond length ($D=0.7$ a.u.) and the dashed line to the energy with the configuration of $D/a=0.2676$ (see Sec. IV B).

IV. STRUCTURAL TRANSITIONS

A. Diatomic to monatomic transition

At high pressure we find a first-order structural phase transition from the diatomic molecular phase to a monatomic metallic phase. A comparison of the total energies of both phases makes it possible to predict the transition volume and corresponding pressure. The solid line in Fig. 6 denotes the total energy of molecular hydrogen with the value of D fixed at the molecular bond length. Since the energy differences between the structures are very small, we show relative energy differences referenced to the metallic hcp structure which is the stable monatomic phase near $r_s = 1.0$ a.u.⁴ Our results for the monatomic metallic phases indicate that the simple cubic (sc) structure is most stable in the low-pressure region, that the hcp and bcc phases become more stable with increasing pressure, and that the fcc phase is always the highest in energy. The transition volume and pressure in the transition from sc to hcp are $r_s = 1.25 \pm 0.05$ and $p \sim 4.4$ Mbar, respectively. As expected and discussed in our previous report,⁴ the sc structure cannot be observed due to the more stable molecular Pa_3 structure and a structural transition occurs between the Pa_3 and the hcp phase at $r_s = 1.2 \pm 0.1$ a.u., which is close to the transition point from sc to hcp.

In order to predict the transition pressure, we fit the value of our total energies to the random-phase-approximation formula for the uniform electron gas—as was done in our previous paper.⁴ However, when we fit the energy values over the whole range of r_s , it is very hard to obtain an accurate fit. Restricting the region of r_s allows us to have an rms error of 1 mRy to our fit in the high-density transition region. Using this interpolation formula, we obtain the pressure and Gibb's free energy, which are to be compared with those of the monatomic metallic phases. Table I provides the total energy and pressure as a function of r_s in the high-density region of the Pa_3 structure. The structural transition from the Pa_3 to the hcp phase occurs at $p = 4 \pm 1$ Mbar with about a 4% volume change. This transition pressure is rather large and beyond current experimental static pressure limits.

TABLE I. Energy and pressure as a function of the electron density, r_s . The bond length is fixed to be that of the free molecule (1 a.u. of pressure is 147.08 Mbar).

r_s	Energy (Ry)	Pressure (a.u.)	Pressure (Mbar)
0.8	-0.178	0.558	82.0
0.9	-0.528	0.264	38.9
1.0	-0.742	0.133	19.6
1.1	-0.877	0.071	10.4
1.2	-0.964	0.039	5.8
1.3	-1.023	0.023	3.3
1.4	-1.064	0.014	2.0
1.5	-1.092	0.009	1.2
1.6	-1.113	0.005	0.8
1.7	-1.128	0.004	0.5
1.8	-1.140	0.002	0.4

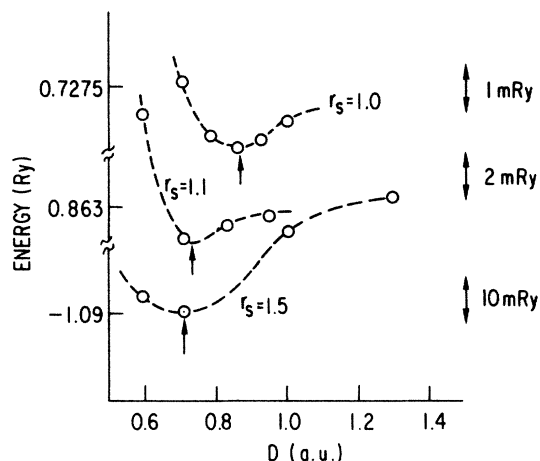


FIG. 7. Total energy of molecular hydrogen in the Pa_3 structure as a function of the half bond length for different r_s values.

B. Relaxation of the interproton bond length

Up to now we have assumed that the interproton bond length $2D$ is constant as a function of pressure. It is expected, however, that the bond length changes beyond a certain pressure due to the change in the electron distribution. With increasing pressure, the distribution of the electrons becomes more uniform, resulting in a weakening of the covalent bonding interactions between the protons in a H_2 molecule.

In order to investigate this effect, we performed total energy calculations with varying bond length for certain r_s values. The results in Fig. 7 indicate that, indeed, the bond length changes beyond a pressure corresponding to $r_s = 1.1$ a.u. At low pressure, we are very close to the experimental hydrogen molecule bond length and this value is stable up to $r_s = 1.1$ a.u. Beyond this density the bond length starts to increase. We expect, however, that this increase is limited up to the distance corresponding to $D/a = 0.2676$, at which $2D$ becomes the same as the next-nearest-neighbor interproton distance. The Madelung energy contribution is lowest in this configuration. We give in Table II the Madelung constant α_M for several values of D/a in the Pa_3 structure. When $D/a = \sqrt{3}/4$, the Pa_3 structure corresponds to the sc structure. Since the Madelung energy ($-\alpha_M/r_s$) determines the stable structure at very high densities, the bond length will eventually follow the rule $D/a = 0.2676$ with increasing pressure.

The dashed curve in Fig. 6 shows the total energy as a function of the density for $D/a = 0.2676$. The intersection of the solid and dashed curve near $r_s = 1.1$ a.u. indicates that relaxation of the bond length will start in this region. Actually, the transition from $D = 0.70$ to $D/a = 0.2676$ is sharp as is seen in the top of Fig. 8. The calculated bond length at $r_s = 1.0$ a.u. already obeys $D/a = 0.2676$ and it decreases afterwards with pressure following $D/a = 0.2676$. Interestingly, near $r_s = 0.81$ a.u., the equilibrium bond length with the configuration

TABLE II. Madelung constant α_M for values of D/a in the Pa_3 structure. For comparison, the Madelung constants of the other monatomic structures are also given.

Pa_3 structure	D/a	α_M
	$\sqrt{3}/4$	1.760 12
	$\sqrt{2}/4$	1.769 54
	0.3	1.781 36
	0.2676	1.784 67
	0.25	1.782 77
	0.2	1.746 31
	0.1	1.196 08
	0.05	0.282 83
bcc		1.791 86
fcc		1.791 75
hcp		1.791 68
sc		1.760 12
Diamond		1.670 12

$D/a = 0.2676$ is 0.7 a.u., which is the same as that of a free molecule. Hence the total energy curves of both configurations, $D = 0.7$ and $D/a = 0.2676$, intersect again at this density, but they do not cross. As already seen in Fig. 6, the total energy of Pa_3 hydrogen for fixed D has an intriguing structure in that the difference in energy from the hcp values is clearly nonparabolic. These deviations from a second-order polynomial are related to the complicated variations of the distance of a hydrogen nucleus in one molecule to hydrogen nuclei in the other molecules, which results in an inflection point in the total energy

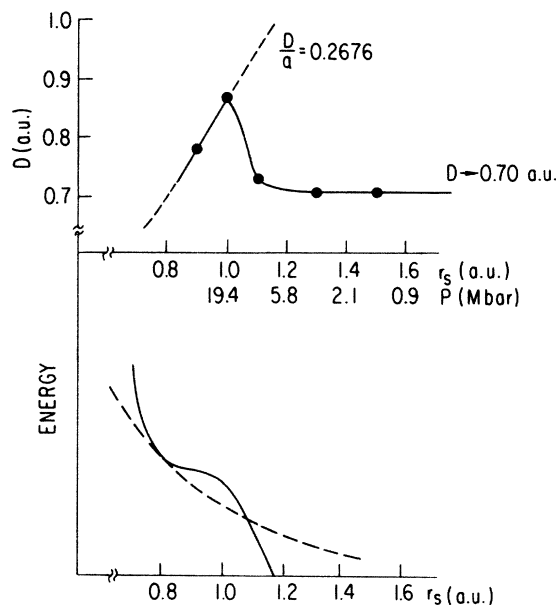


FIG. 8. Upper panel: bond relaxation as a function of r_s . Points are computational results. The broken line represents the bond length satisfying the relation $D/a = 0.2676$. Lower panel: general shape of the total energy of Pa_3 solid H_2 . The solid line represents the total energy curve with fixed bond length ($D = 0.7$) and the dashed line corresponds to the configuration $D/a = 0.2676$.

near $r_s = 0.9$ a.u. The lower part of Fig. 8 shows this in a qualitative way; we plot the total energy of the Pa_3 structure with D fixed (solid line) and D/a fixed (dashed line). Because the energy differences are small compared to the overall change in total energy, these lines are indistinguishable as the latter scale; we therefore show this difference only schematically. It is seen that the energy with D fixed increases with increasing pressure, and that a curvature change occurs. Hence, there occurs another intersection between the two curves near $r_s = 0.81$ a.u., in addition to the crossing near $r_s = 1.1$ a.u.

It should be noticed that the relaxation of the bond length occurs for $r_s < 1.1$ a.u. and it does not affect the structural transition discussed in the last section. This is clearly seen in Fig. 6 where the total energy curve for $D/a = 0.2676$ (dashed line) is always above the hcp values. Additionally, at $r_s = 1.2$ a.u. our results show that the bond length D still has the molecular value.

V. DISCUSSION

We have performed precise first-principles FLAPW band-structure and total-energy calculations for both monatomic and diatomic solid hydrogen in order to investigate the structural transition between these phases. As mentioned earlier, the numerical error in the low-density insulating region is rather large because of the very small value of the muffin-tin radius required and the limit on the number of basis functions, which is governed by computer time and memory. The dependence of the total energy on the number of basis functions should be treated very carefully in this region to get reasonable precision. On the other hand, in the high-density metallic region the dependence of the total energy on the number of k points is much more important than that on the number of basis functions. As discussed in the Appendix, a converged value of the total energy is obtained using an extrapolation scheme based on the analytical error behavior of the linear tetrahedron method. This leads to a better than 1 mRy precision in the total energy in the high-density metallic region. It should be mentioned, however, that the value of the transition pressure is very sensitive to the errors in the total energy and the extrapolation used. Our total uncertainty in the transition pressure from the Pa_3 structure to the hcp structure is around 1 Mbar.

Up to now we only have considered static lattices of all phases. Due to the quantum solid nature of solid hydrogen, however, the zero-point motion of the protons plays an important role in the determination of the stable structure, as discussed by Chakravarty *et al.*¹² A characteristic of quantum solids, which solid hydrogen shares with solid helium, is a large compressibility because the particles are not located at the minimum of the attractive potential well of the neighbors, and anharmonic effects become very important. Thus, an approach such as the self-consistent harmonic phonon approximation¹⁴ is essential for the study of the lattice dynamics of quantum solids.

Phonon effects increase the overall total energies of both phases of solid hydrogen. It is expected that the effect is larger in the high-density region in both cases, since

the energy from the proton motion is inversely proportional to r_s . Quantitative conclusions about the effects of the phonons on the transition pressure can only be drawn by including the consistent and elaborate methods of lattice dynamics for both systems. The results of Chakravarty *et al.*,¹² however, suggest that the corrections are similar but somewhat larger in the diatomic phase; thus our value of the transition pressure is expected to be an upper bound for the real theoretical value including phonon effects.

There occur two different transitions at high pressure. The first, an electronic transition, is a pressure-induced metallization by band overlap in the diatomic molecular phase which occurs without a structural change, and the second is a structural transition from the diatomic to a monatomic phase. The first is a second-order phase transition and the second is a first-order phase transition. A molecular metallic phase exists for densities with $1.2 < r_s < 1.44$ a.u. It is expected that all the other molecular solids, for example N_2 , O_2 , and especially I_2 , behave in a similar way.¹⁵ The calculations on these systems will be easier to perform than in the hydrogen system because of the much larger values of D/a .

Bond relaxation has been discussed before by many authors.¹⁶ While the general trends in our results are similar to previous results, the density at which relaxation sets in is somewhat different. For example, Wood and Ashcroft¹⁶ also predict that the bond length $2D$ will follow the rule of $D/a = 0.27$ in the high-density limit, but they find that the density at which $2D$ increases above the value of the hydrogen molecule is $r_s = 2.8$ a.u. In our results the molecular bond length is maintained down to $r_s \sim 1.1$ a.u. Between $r_s = 1.1$ and 1.0 a.u., the value of D increases rapidly and reaches the high-density prediction at $r_s = 1.0$ a.u.

Among the monatomic metallic structures we have studied, the simple cubic phase has the lowest total energy for $r_s > 1.3$ a.u. In general, however, paramagnetic simple cubic structures are not supposed to be stable and it is expected that the formation of either a charge-density wave (CDW) or spin-density wave (SDW) will destroy the symmetry of this state. Our results indicate that in the low-density limit,¹⁷ the antiferromagnetic sc phase has a lower total energy and this shows the instability of the paramagnetic simple cubic phase with respect to the formation of a SDW in the low-density limit ($r_s \geq 3.0$ a.u.). Magnetic instabilities do not occur at the densities considered in this paper. There are, of course, structural instabilities because molecular phases have a lower energy for $r_s > 1.3$ a.u. In this respect it is interesting that the sc structure is a special case of the Pa_3 space group, with $D/a = \sqrt{3}/4$. Table II indicates that the Madelung contribution to the total energy favors distortions of the sc structure which decrease D/a . This is in agreement with a general observation for other systems that a simple cubic structure is often unstable with respect to distortions.¹⁸ The stability of solid molecular hydrogen indicates that in this case the sc phase is unstable with respect to a $\langle 111 \rangle$ CDW dimerization, similar to the mechanism of a Peierls distortion. Thus the simple cubic hydrogen system is an interesting example showing both CDW and SDW phase transitions.

ACKNOWLEDGMENTS

We thank D. J. Kim, T. Oguchi, A. K. McMahan, M. Ross, and R. Monnier for helpful discussions. This work was supported by the Air Force Office of Scientific Research (Grant No. 81-0024), by the Department of Energy, and by a computing grant from Cray Research, Inc.

APPENDIX

The small values of the energy differences between the different structures require a careful consideration of the numerical parameters which affect the total energy and a careful analysis of their convergence tests. The numerical parameters to be checked for each system are (i) the number of nonspherical terms in the representation of potential and charge density inside the muffin-tin spheres, (ii) the number of plane waves in the representation in the interstitial region, (iii) the energy parameters which enter into the LAPW calculations, (iv) the number of basis functions, and (v) the number of k points in the irreducible wedge of the Brillouin zone carried in the self-consistent cycles. In the band-structure calculations on solid hydrogen we have found that, as usual, the most important parameters are the number of basis functions and k points. In the following we show the effect of all these parameters separately.

(i) Nonspherical terms. It is expected that this effect is more important in the low-density insulating region since the density becomes uniform in the high-density limit. We performed total energy calculations including terms up to $l=3$ or $l=4$ at $r_s=3.1$ a.u. The number of nonspherical terms (Kubic harmonics) is 6 for $l=3$ and 9 for $l=4$. The change in total energy upon including terms up to $l=4$ is negligible (less than 0.1 mRy) and hence we only included terms up to $l=3$ in most of our calculations.

(ii) Number of plane waves for representing the interstitial potential. This parameter is chosen in such a way that all contributions of reciprocal-lattice vectors used in the set of basis functions are incorporated into the expansion of the charge density in the interstitial region. In the potential, however, larger lattice vectors are important, and, therefore, the number of plane waves as defined in the previous sentence is only a minimal value. In the case of molecular hydrogen at $r_s=3.1$ a.u., the use of this minimal value of the number of plane waves still results in an error of 156 mRy in the total energy. In the actual calculations at $r_s=3.1$ a.u. we had to use more than 6000 plane waves (more than 190 stars) in order to describe the

TABLE III. Dependence of the total energy on the number of basis functions (NB) for solid molecular hydrogen at $r_s=3.1$ a.u.

RK_{\max}	NB	$E_{\text{tot}}(\text{Ry})$
1.785	257	-1.0603
1.996	389	-1.0851
2.232	515	-1.1033
2.404	691	-1.1121
2.525	751	-1.1166

TABLE IV. Extrapolation of the total energy as a function of RK_{\max} at $r_s=3.1$ a.u.; $E=E_0+a/(RK_{\max})^n$.

n	a	E_0 (Ry)	ΔE (Ry)
2	0.3610	-1.1746	0.0011
3	0.4981	-1.1478	0.0002
4	0.7637	-1.1346	0.0009
5	1.2345	-1.1478	0.0017

potential sufficiently accurately (errors in total energy less than 1 mRy).

(iii) Energy parameters. These parameters, inherent to linear band methods,¹⁹ give the values of the energy at which the radial functions and the energy derivatives of the radial functions are calculated. They are usually chosen at the center of the occupied band. In the case of solid hydrogen, the sensitivity with respect to the choice of energy parameters is small; even when we change the position of the energy parameters by 0.6 Ry, the total energy is changed by less than 1 mRy.

(iv) Number of basis functions. This parameter depends on the ratio of the interstitial volume and the total volume. Since this ratio is very large in the case of low-density molecular solid hydrogen, the effects of this parameter are very important. The number of basis functions is conveniently determined by the quantity RK_{\max} , which is the product of the muffin-tin radius and a sphere radius K_{\max} in reciprocal space. For a given point \mathbf{k} , our basis set includes all reciprocal-lattice vectors \mathbf{G} with $|\mathbf{G}-\mathbf{k}| < K_{\max}$. In close-packed metals good precision for the total energy is usually obtained with $RK_{\max} > 8$. The dependence on the number of basis functions at $r_s=3.1$ is given in Table III. Because of the small muffin-tin radius, the dependence on this parameter is very large and the converged value of the total energy will be far from the results in Table III. Hence we should have to obtain the converged value using an assumed power-law behavior³ for the error as a function of RK_{\max} , see Table IV, such as $E=E_0+a(RK_{\max})^{-n}$.

The resulting variations of the total energy are very large. For example, if we choose the average of the values with $n=3$ and 4 then $E_0=1.1412\pm 0.0093$ (large uncertainty of ~ 10 mRy). Hence our errors are large in the low-density region. In contrast to this behavior, the results in the high-density metallic region at $r_s=1.0$ a.u. show negligible dependence on this parameter, see Table V. Due to the small size of the interstitial region in this case the effects are negligible. Hence sufficiently con-

TABLE V. Dependence of the total energy on the number of basis functions (NB) in high-density metallic hydrogen for $r_s=1.0$ a.u.

RK_{\max}	NB	E_{tot}
4.793	257	-0.6920
5.534	389	-0.6921
6.188	515	-0.6921
7.452	691	-0.6921

TABLE VI. Variation of the total energy on the number of k points (N_k) used for two extreme values of r_s .

$r_s = 3.1$		$r_s = 1.0$	
N_k	E_{tot} (Ry)	N_k	E_{tot} (Ry)
20	-0.9240	20	-0.7057
40	-0.9241	40	-0.7189
80	-0.9242	80	-0.7273

verged results with respect to RK_{max} are easily obtained in the high-density region where the phase transitions take place.

(v) Number of k points. This parameter becomes important since we employ the analytic linearized tetrahe-

dron method for the integrals in reciprocal space, which appear in the construction of the charge-density and the total energy. It depends critically on the Fermi surface topology. Hence the effects are only important in the metallic phase and are small in the insulating phase. In Table VI we show the variation of the total energy with the number of k points for two extreme values of r_s .

These results indicate that indeed the effect is negligible in the insulating phase ($r_s = 3.1$ a.u.), while the effect is very important in the metallic phase ($r_s = 1.0$ a.u.). In the linearized tetrahedron method, the error in total energy scales³ with $N_k^{(-2/3)}$ (N_k is the number of k points). From this behavior of E_{tot} as a function of N_k we obtain a converged value of the total energy $E_0 = -0.7414 \pm 0.0005$ at $r_s = 1.0$ a.u.

*Present address: Department of Physics, Oregon State University, Corvallis, OR 97331-6507.

¹E. Wigner and H. B. Huntington, *J. Chem. Phys.* **3**, 764 (1935).

²For a recent review, see, I. F. Silvera, *Rev. Mod. Phys.* **52**, 393 (1980); J. van Kranendonk, *Solid Hydrogen Physics* (Plenum, New York, 1983).

³H. J. F. Jansen and A. J. Freeman, *Phys. Rev. B* **30**, 561 (1984).

⁴B. I. Min, H. J. F. Jansen, and A. J. Freeman, *Phys. Rev. B* **30**, 5076 (1984).

⁵K. Takemura, S. Minomura, O. Shimomura, and Y. Fujii, *Phys. Rev. Lett.* **45**, 1881 (1980).

⁶P. Hohenberg and W. Kohn, *Phys. Rev.* **136**, B864 (1964); W. Kohn and L. J. Sham, *Phys. Rev.* **140**, A1133 (1965).

⁷L. Hedin and B. I. Lundqvist, *J. Phys. C* **4**, 2064 (1971).

⁸M. Weinert, E. Wimmer, and A. J. Freeman, *Phys. Rev. B* **26**, 4571 (1982).

⁹C. Friedli and N. W. Ashcroft, *Phys. Rev. B* **16**, 662 (1977).

¹⁰P. Giannozzi and S. Baroni, *Phys. Rev. B* **30**, 7187 (1984).

¹¹K. Inoue, H. Hanzaki, and S. Suga, *Solid State Commun.* **30**, 627 (1979); A. Gedanken, B. Raz, and J. Jortner, *J. Chem. Phys.* **59**, 2752 (1973).

¹²S. Chakravarty, J. H. Rose, D. Wood, and N. W. Ashcroft, *Phys. Rev. B* **24**, 1624 (1981).

¹³D. A. Liberman, *Int. J. Quantum Chem. Symp.* **10**, 297 (1976), and Ref. 12.

¹⁴N. S. Gillis, N. R. Werthamer, and T. R. Koehler, *Phys. Rev.* **165**, 951 (1968).

¹⁵A. K. McMahan and R. Lesar, *Phys. Rev. Lett.* **54**, 1929 (1985); M. Ross, *Rep. Prog. Phys.* **48**, 1 (1985), and references therein.

¹⁶D. M. Wood and N. W. Ashcroft, *Phys. Rev. B* **25**, 2532 (1982), and references therein.

¹⁷B. I. Min, T. Oguchi, H. J. F. Jansen, and A. J. Freeman, *Phys. Rev. B* **33**, 324 (1986).

¹⁸R. M. Martin (private communication).

¹⁹O. K. Andersen, *Phys. Rev. B* **12**, 3060 (1975).